JGS
Journal of the Geological Society

Research article

Published online April 17, 2018 https://doi.org/10.1144/jgs2017-120 | Vol. 175 | 2018 | pp. 594–604

Magnetostratigraphy of the Toarcian Stage (Lower Jurassic) of the Llanbedr (Mochras Farm) Borehole, Wales: basis for a global standard and implications for volcanic forcing of palaeoenvironmental change

Weimu Xu[1]*, Conall Mac Niocaill[1], Micha Ruhl[1], Hugh C. Jenkyns[1], James B. Riding[2] & Stephen P. Hesselbo[3]

[1] Department of Earth Sciences, University of Oxford, Oxford OX1 3AN, UK
[2] British Geological Survey, Keyworth, Nottingham NG12 5GG, UK
[3] Camborne School of Mines and Environment and Sustainability Institute, University of Exeter, Penryn Campus, Penryn TR10 9FE, UK

W.X., 0000-0002-3239-0272; C.M., 0000-0002-3782-0198; M.R., 0000-0001-8170-0399; H.C.J., 0000-0002-2728-0984; J.B.R., 0000-0002-5529-8989; S.P.H., 0000-0001-6178-5401

* Correspondence: weimu.xu@earth.ox.ac.uk

Abstract: The Lower Jurassic Toarcian Stage (*c.* 183–174 Ma) is marked by one of the largest global exogenic carbon-cycle perturbations of the Phanerozoic, which is associated with the early Toarcian Oceanic Anoxic Event (T-OAE; *c.* 183 Ma). Climatic and environmental change at the T-OAE is reasonably well constrained in the marine realm, with marine anoxic or euxinic conditions developing locally across both hemispheres, at the same time as the T-OAE negative carbon-isotope excursion. However, high-resolution stratigraphic comparison between different palaeo-ocean basins and with the continental realm can be complicated. Palaeomagnetic reversals can provide a precise and accurate stratigraphic correlation tool between marine and continental sedimentary archives, and even between sedimentary and igneous successions. Here, we present a high-resolution magnetostratigraphic record for the Toarcian Stage in the biostratigraphically complete and expanded Llanbedr (Mochras Farm) Borehole, Cardigan Bay Basin, Wales. This study provides the first geomagnetic polarity reversal scale that is integrated with high-resolution biostratigraphy and carbon-isotope stratigraphy for the entire Toarcian Stage. This stratigraphic framework also provides a new, precise correlation with the basalt lava sequence of the Karoo–Ferrar Large Igneous Province, linking the Pliensbachian–Toarcian boundary and T-OAE climatic and environmental perturbations directly to this episode of major volcanic activity.

Supplementary material: Details of the palaeomagnetic data and dip direction are available at https://doi.org/10.6084/m9.figshare.c.4052720

Received 8 October 2017; **revised** 13 February 2018; **accepted** 15 February 2018

The Toarcian, the final stage of the Early Jurassic, has an estimated duration of 8.3–8.6 myr (2014 Geological Time Scale; Boulila *et al.* 2014), with the Pliensbachian–Toarcian boundary dated at *c.* 183.6 Ma (Pálfy & Smith 2000). The early Toarcian was marked by the widespread development of anoxic or euxinic conditions that led to substantial organic-carbon burial, an event termed the Toarcian Oceanic Anoxic Event (T-OAE). This palaeoceanographic phenomenon is recognized as one of the most intense and geographically extensive events of oceanic redox change and accompanying organic-carbon burial in the Mesozoic (Jenkyns 1985, 1988, 2010). The T-OAE is marked by major changes in global geochemical cycles (e.g. Os, S, Sr), with an apparently rapid *c.* 7‰ negative shift in marine and terrestrial organic-carbon isotope records and a smaller (3–6‰) negative excursion in carbonate and compound-specific archives (Hesselbo *et al.* 2000, 2007; Sælen *et al.* 2000; Schouten *et al.* 2000; Jenkyns *et al.* 2002; Cohen *et al.* 2004; Kemp *et al.* 2005; Hermoso *et al.* 2009; Al-Suwaidi *et al.* 2010, 2016; Gill *et al.* 2011; Newton *et al.* 2011; French *et al.* 2014; Suan *et al.* 2015; McArthur *et al.* 2016; Percival *et al.* 2016; Xu *et al.* 2017, 2018).

The observed early Toarcian perturbation to the exogenic carbon cycle has been linked to volcanic activity associated with the Karoo–Ferrar Large Igneous Province and associated release of volcanogenic carbon dioxide (CO_2), thermogenic methane (CH_4) and CO_2 from sill intrusion into Gondwanan coals and shales, and biogenic methane from dissociation of sub-seafloor clathrates (Duncan *et al.* 1997; Hesselbo *et al.* 2000; Kemp *et al.* 2005; McElwain *et al.* 2005; Svensen *et al.* 2007; Percival *et al.* 2015). The Pliensbachian–Toarcian boundary was also marked by global carbon-cycle change, with a *c.* 2–3‰ negative carbon-isotope excursion (CIE) in marine carbonate, organic matter and fossil wood (Hesselbo *et al.* 2007; Littler *et al.* 2010; Bodin *et al.* 2016; Percival *et al.* 2016). An elevated atmospheric pCO_2-induced global temperature increase in the ocean–atmosphere system is credited with causing disruption of marine ecosystems as well as enhanced hydrological cycling and continental weathering on land (Cohen *et al.* 2004; Danise *et al.* 2013, 2015; Ullmann *et al.* 2014; Korte *et al.* 2015; Percival *et al.* 2016; Rita *et al.* 2016; Martindale & Aberhan 2017).

Stratigraphic studies of the Toarcian have primarily focused on the lower part of the stage, specifically on the T-OAE interval, utilizing bio- and chemostratigraphy. Magnetostratigraphic study of the Toarcian Stage has been confined to only a few localities. These include the Breggia Gorge in southern Switzerland (Horner & Heller 1983), Thouars and Airvault in France (Galbrun *et al.* 1988), the Iberian Range and Iznalloz in Spain (Galbrun *et al.* 1990; Osete *et al.* 2007; Comas-Rengifo *et al.* 2010), and the Neuquén Basin in Argentina (Iglesia Llanos & Riccardi 2000). Additionally, an extended magnetostratigraphic record, spanning the Pliensbachian to earliest Cretaceous interval, was obtained from the Northern Apennines in Italy (Satolli *et al.* 2015), but ammonite biostratigraphy is relatively poorly constrained in this succession. Palaeomagnetic data from the lower and middle

Toarcian in the Iberian Range were subsequently synthesized (Osete *et al.* 2007; Comas-Rengifo *et al.* 2010) and adopted for the Geological Time Scale 2012 (GTS2012; Ogg & Hinnov 2012).

Few existing magnetostratigraphic records cover the upper Toarcian. Furthermore, sampling resolution in this interval is commonly relatively low, affected by hiatuses, or the ammonite biostratigraphy is not well defined. The use of magnetostratigraphy for Toarcian stratigraphic correlation has also been relatively restricted because no published record integrates magnetostratigraphy with both (ammonite) biostratigraphy and carbon-isotope chemostratigraphy for the entire Stage. Arguably, the best example of an integrated Toarcian stratigraphy is a high-resolution magnetostratigraphy combined with carbon-, oxygen- and strontium-isotope data in the biostratigraphically well-constrained Almonacid De La Cuba Section in NE Spain (Comas-Rengifo *et al.* 2010; da Rocha *et al.* 2016), but these investigations were confined to the Pliensbachian–Toarcian transition. An integrated stratigraphy for the T-OAE interval, using the aforementioned proxies, has not hitherto been presented.

The Llanbedr (Mochras Farm) Borehole, hereafter referred to as Mochras, drilled in the Cardigan Bay Basin, west Wales, UK, recovered a Lower Jurassic succession that combines unusual thickness with relative biostratigraphic completeness (Woodland 1971; Dobson & Whittington 1987; Hesselbo *et al.* 2013; Copestake & Johnson 2014; Ruhl *et al.* 2016). The *c.* 260 m thick Toarcian succession is much thicker than in other coeval European core and outcrop successions, and is generally characterized by periodic alternations between limestone and (marly) mudstone (Hesselbo *et al.* 2013; Ruhl *et al.* 2016; Xu *et al.* 2018). The Toarcian interval of the Mochras core comprises eight ammonite zones and nine ammonite subzones (Page 2003; Copestake & Johnson 2014); the *aalensis* Zone at the top of the Toarcian is probably truncated in the Mochras core (Ivimey-Cook 1971). The ammonite zones and subzones are referred to as zones and subzones hereafter, and are named by a typifying species name (e.g. the *tenuicostatum* Zone). Furthermore, five foraminiferal zones are also resolved (Copestake & Johnson 2014).

Carbon-isotope analyses of bulk organic matter show an overall positive excursion of 3–4‰ in $\delta^{13}C_{TOC}$, relative to upper Pliensbachian and upper Toarcian values of −27 to −28‰, which spans the Upper Pliensbachian upper *spinatum* Zone to Toarcian middle *bifrons* Zone (Jenkyns & Clayton 1997; Jenkyns *et al.* 2001; Katz *et al.* 2005; van de Schootbrugge *et al.* 2005; Xu *et al.* 2018). This early Toarcian long-term positive trend in $\delta^{13}C_{TOC}$, presumably linked to the globally significant burial of isotopically depleted organic carbon, is interrupted by the major negative CIE in marine and terrestrial organic matter and marine calcite that typically marks the main phase of the T-OAE. The negative CIE in the Mochras core is recorded as a distinct >7‰ and *c.* 6.5‰ negative shift in bulk $\delta^{13}C_{TOC}$ and $\delta^{13}C_{CARB}$, respectively (Jenkyns & Clayton 1997; Jenkyns 2003; van de Schootbrugge *et al.* 2005; Xu *et al.* 2018). A pilot study on the Mochras core proved the feasibility of a magnetic-polarity study on this expanded and bio- and chemostratigraphically well-constrained sedimentary archive (Hesselbo *et al.* 2013). Here, we present the first high-resolution magnetostratigraphic record for the complete Toarcian Stage and use it to construct an integrated Toarcian stratigraphic framework. The integrated stratigraphic data presented here provide a reference framework for correlation between Toarcian marine and continental sedimentary basins worldwide. This study also allows stratigraphic correlation between the T-OAE and associated climatic and environmental change, and volcanic activity in the Karoo–Ferrar Large Igneous Province.

Geological setting

The sediments recorded in the Toarcian strata of the Mochras core were deposited at a palaeo-latitude of *c.* 35–40°N, at the southern end of the transcontinental seaway and at the northwestern end of the Tethys Ocean (Fig. 1; Torsvik *et al.* 2012; Hesselbo *et al.* 2013; Müller *et al.* 2016). The Cardigan Bay Basin Jurassic strata are downthrown against the Lower Palaeozoic Welsh Massif along a major normal fault system, comprising the Mochras, Tonfanau and Bala faults at the eastern and southeastern margins of the basin (Tappin *et al.* 1994). The Mochras Borehole was drilled onshore by the British Geological Survey (BGS) and UCW Aberystwyth (now Aberystwyth University) from 1967 to 1969, on the coast of Cardigan Bay, in NW Wales (Woodland 1971; Dobson & Whittington 1987; Hesselbo *et al.* 2013; Copestake & Johnson 2014). The core penetrates the entire Lower Jurassic in the Cardigan Bay Basin (with only the *aalensis* Zone at the top of the Toarcian probably truncated in the Mochras core), which is underlain by Triassic and overlain, unconformably, by Cenozoic and Quaternary successions. The Lower Jurassic in this borehole has a remarkable thickness of *c.* 1300 m, much greater than coeval onshore sections in other parts of the UK and continental Europe (see fig. 2 of Ruhl *et al.* 2016), recording a sustained high sedimentation rate. The relatively homogeneous lithology dominated by argillaceous sediments with alternating muddy limestones, marls and mudstones indicates a relatively open- and deep-marine (hemipelagic) setting (Sellwood & Jenkyns 1975).

Lithologically, the Toarcian in the Mochras core is dominated by metre-scale carbonate-rich mudstone to carbonate-poor mudstone alternations. The *falciferum* Zone in the succession is generally carbonate-poor and is marked by several distinct, small-scale (10^0–10^1 cm) intervals of coarser grained deposits that are rich in macroscopic wood fragments and sedimentary structures such as wave ripples and soft-sediment deformation (Xu *et al.* 2018). X-ray diffraction (XRD) analyses on the Toarcian strata in the Mochras core reveal abundant quartz, calcite, chamosite, illite and mica, and illite-rich illite–smectite minerals, together with small amounts of kaolinite, K-feldspar, plagioclase, Fe-dolomite, siderite and pyrite (Xu *et al.* 2018).

Materials and methods

The Mochras slabbed core (in 1 m core-lengths) is stored in boxes at the British Geological Survey, Keyworth, Nottingham, UK, at normal atmospheric conditions. The Toarcian Stage in the Mochras borehole occurs over the depths of 863.50–601.83 m. The core was drilled vertically, with the bedding dipping gently (of the order of 10°) to the east (Tappin *et al.* 1994; Hesselbo *et al.* 2013; see also the Supplementary Material). The core slabs of the Toarcian are reasonably well preserved (*c.* 96% are present in the archive half of the section), especially in comparison with the Hettangian and Sinemurian intervals, for which material is only patchily available (Hesselbo *et al.* 2013; Ruhl *et al.* 2016; Xu *et al.* 2018). Core samples are not affected by drilling-induced formation of biscuits (see Pearson & Thomas 2015). The diameter of the whole Mochras core ranges from 10 to 15 cm (Woodland 1971). The surface of the Toarcian core slab is *c.* 10 cm wide. Samples for magnetic-polarity analysis were selected at 2–5 m resolution, spanning the entire Toarcian interval (except that the *aalensis* Zone is partially truncated owing to unconformity) in the Mochras Borehole, from 601.83 to 863.5 m below surface (mbs). In total, 148 cubes (each 2.3 cm × 2.3 cm × 2.3 cm; ~12 cm^3) were prepared from the core sections, composed predominantly of mudstones with varying concentrations of calcium carbonate.

Measurements of the natural remanent magnetization (NRM) were made using a three-axis 2G cryogenic magnetometer, housed in a magnetically shielded room at the University of Oxford palaeomagnetic laboratory. Specimens were stepwise demagnetized using progressive alternating field (AF) techniques through at least 12 steps (up to a maximum of 100 mT), until they became unstable.

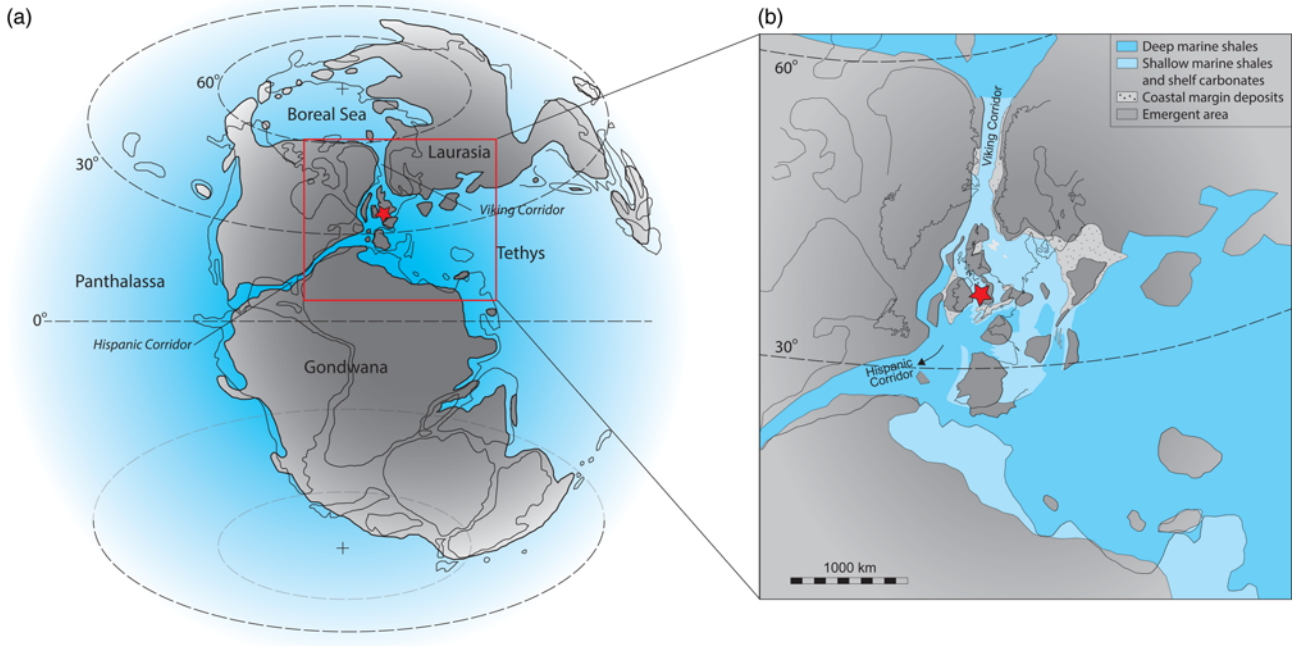

Fig. 1. Geographical maps. (**a**) Early Jurassic global palaeogeography, modified after Dera *et al.* (2011), Korte *et al.* (2015) and Ruhl *et al.* (2016). (**b**) Detail of the area within the red square in (**a**). The red star indicates the palaeogeographical position of the Mochras Borehole.

The AF technique was used so as to retain the material for geochemical and biostratigraphical analyses that require unaltered samples. Demagnetization results were plotted on orthogonal and stereographic projections; characteristic remanence components were identified using least-squares algorithms (e.g. Kirschvink 1980). Components were considered stable where they were defined by at least three consecutive points on orthogonal projections and had a maximum angular deviation not exceeding 20°.

Results

The NRM intensities of the measured samples ranged from 0.06 to 1.6 mA m^{-1}, with a mean of 0.26 mA m^{-1}. During progressive AF demagnetization three classes of behaviour were identified: Class A, samples for which demagnetization trajectories tended towards the origin, and lines could be fitted to the demagnetization trajectories (65 samples); Class B, samples for which the polarity could be determined, but with very poor line-fits and maximum angular deviation of >30°, so that no inclination was computed (45 samples; NRM intensities were generally very low); Class C, samples that demonstrated unstable behaviour during demagnetization, or where the NRM intensities were too low to provide meaningful demagnetization data (38 samples). Examples of Class A and B behaviour are given in Figure 2. The magnetostratigraphy constructed here is primarily based on data from Class A samples, but the polarities of Class B samples were used as supporting evidence. Because the original Mochras core is azimuthally unoriented, 'inclination-only' statistics (McFadden & Reid 1982) were conducted on the dataset presented herein. Of the 65 samples with Class A behaviour, 36 yield downward-pointing inclinations, which are interpreted as normal polarity given the northern hemisphere location of the sampling site during the Toarcian. These samples yield a mean inclination of +37.0° ($\alpha95 = 7.4°$; $k = 8.48$). The remaining 29 samples yield negative inclinations, which are interpreted as reversed polarity, with a mean inclination of −37.7° ($\alpha95 = 5.3°$; $k = 18.17$). Normal- and reverse-polarity data thus yield inclinations that are almost identical, and constitute a positive 'inclination-only' reversal test. When both polarities are combined we obtain an overall mean inclination of +37.3 ($\alpha95 = 5.1°$; $k = 11.16$), suggesting a palaeo-latitude of 21°N. The inclination obtained here is considerably shallower than the expected inclinations of *c.* +54–59° for Mochras at *c.* 183 Ma (based on reference palaeo-latitudes of *c.* 35–40°N; Torsvik *et al.* 2012; Müller *et al.* 2016).

The location of the Mochras Borehole has probably not been at palaeo-latitudes south of 35°N since the Toarcian, so it is highly improbable that a multi-polarity remagnetization post-dating deposition of the Mochras succession has overprinted the original signal. Instead, the original remanence has probably undergone inclination shallowing owing to compaction of the mudstone, a well-documented phenomenon in sedimentary rocks (Kodama 2012, and references therein). Correction for this inclination shallowing with a flattening factor (f) of 0.6, which is often taken as a standard value, corrects the apparent palaeo-latitude from 21°N to a 'true' palaeo-latitude of 33°N (Kodama 2012). An alternative f value of 0.5 corrects the apparent palaeo-latitude from 21°N to 38°N, which is within error of the previously reconstructed palaeo-latitudes for this site. Additionally, this inclination shallowing provides a constraint on the age of magnetization as pre-compaction. Hence, the observed inclination shallowing, together with a positive inclination-only reversal test, supports interpretation of the Mochras core palaeomagnetic records as a primary Early Jurassic remanence.

A magnetic-polarity column for the entire Toarcian Stage (albeit only partly covering the *aalensis* Zone, which is probably truncated at the top in the Mochras core) has been constructed (Fig. 3). Identified magnetic polarity in more than one consecutive sample (with at least one Class A sample) is marked by a full-width bar, whereas polarity identified by only one sample (one Class A sample with no Class B sample to support) is marked by a half-width bar (Fig. 3).

Nine normal- and eight reversed-polarity magnetozones were identified and numbered N0–N8 and R0–R7, respectively (Fig. 3). The R0, N4 and N7 magnetozones are based on only one Class A sample and one or two Class B samples as supporting evidence. The N6 magnetozone is a suggestive normal zone based on only Class B

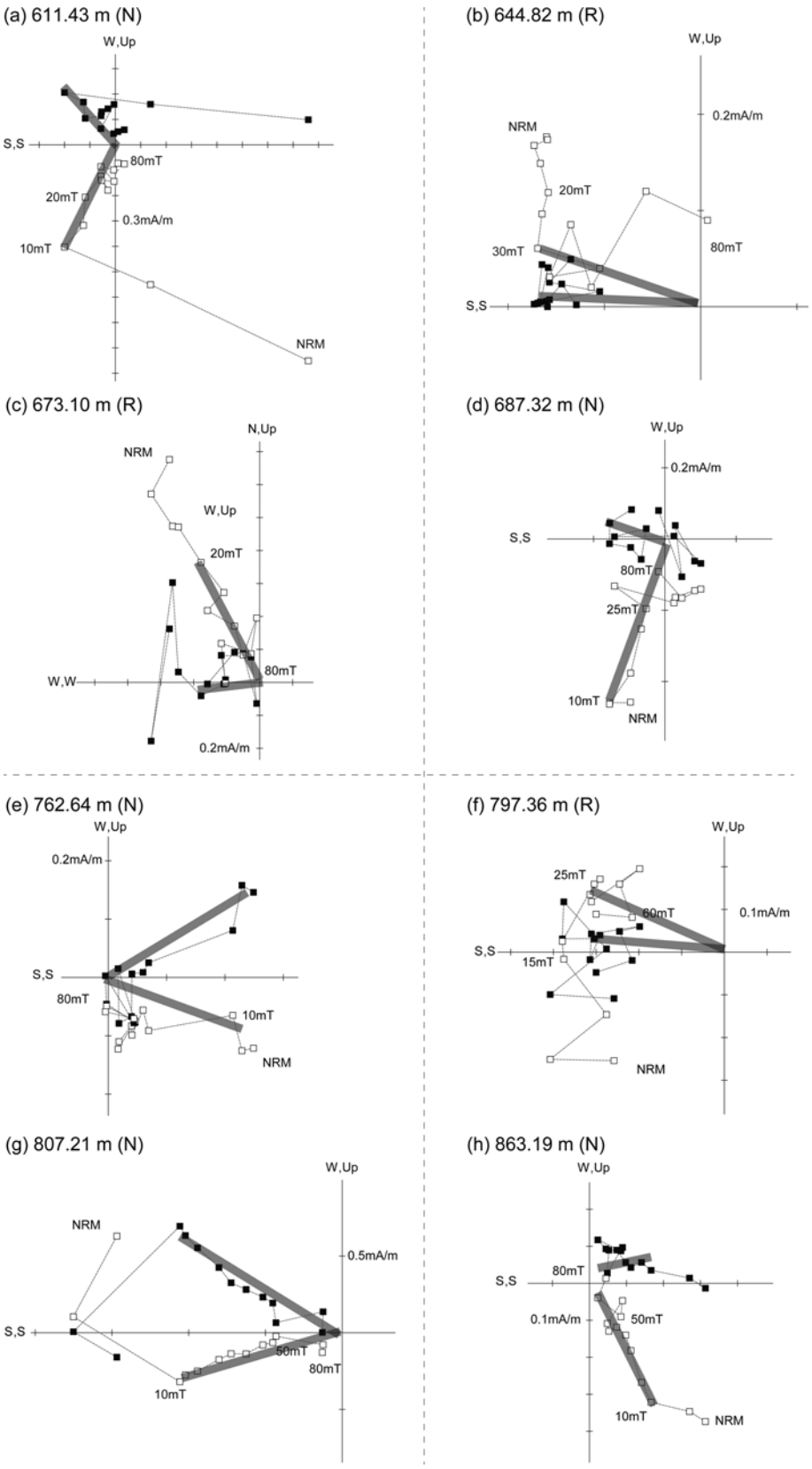

Fig. 2. Orthogonal vector diagrams illustrating the alternating field (AF) demagnetization of eight typical Class A samples from the Toarcian of the Mochras core between 611.43 and 863.19 m (a–h) in stratigraphic order. Samples a, d, e, g and h are normal polarity (N), and samples b, c and f are reversed polarity (R). The closed and open symbols are projections onto horizontal and vertical planes, respectively.

samples and inference from the GTS2012. The interval of normal polarity (N0) probably extends down into the Pliensbachian (Fig. 3). A conservative approach was taken when determining the magnetozones R2 and N3. R2 is based on five Class A samples, although there are two single-specimen normal intervals. N3 is based on two Class A normal samples, but separated by one reverse sample.

Discussion

Magnetostratigraphic correlations

Magnetostratigraphy of the Mochras Borehole can be correlated with other magnetostratigraphic sequences defined in coeval European successions, including the Breggia Gorge section of

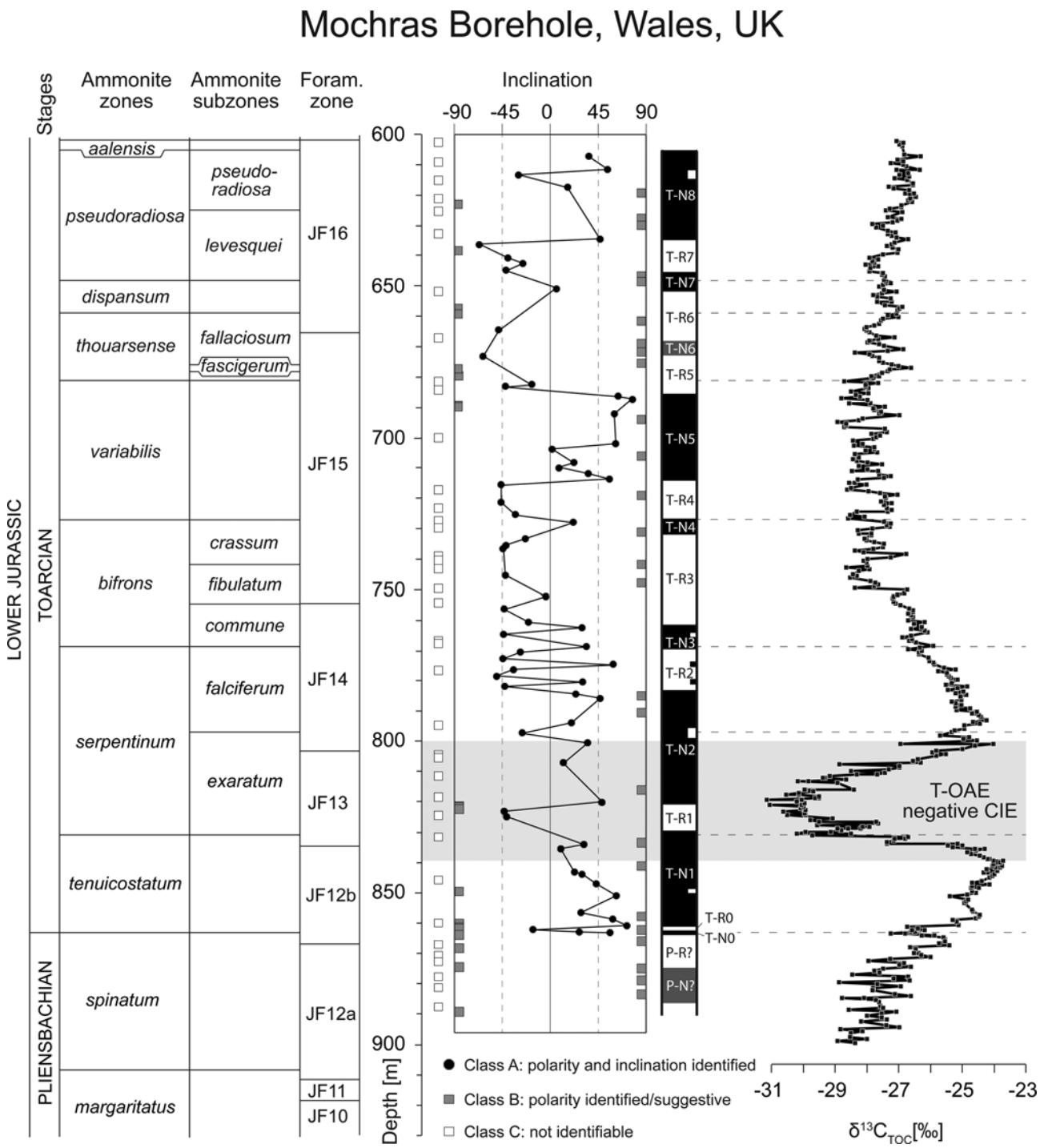

Fig. 3. An integrated synthesis of the stratigraphy of the Toarcian succession in the Mochras Borehole, comprising (ammonite and foraminifer) bio-, carbon-isotope and magnetostratigraphy. The foraminiferal zones are taken from Copestake & Johnson (2014). The inclination values and the magnetostratigraphy column are plotted. The filled black circles represent Class A samples with identified inclinations that form the basis for the construction of the magnetic-polarity record. The dark grey squares represent Class B samples, for which only magnetic polarity was identified; the points at −90° indicate reversed polarity, and the points at 90° indicate normal polarity. The normal-polarity magnetozone is in black and the reversed-polarity magnetozone is in white. The grey zones in the magnetic record indicate magnetozones defined as normal-polarity, only based on (at least two) Class B normal-polarity samples.

southern Switzerland (Horner & Heller 1983) and a number of sections in Spain (Galbrun *et al.* 1990; Osete *et al.* 2007; Comas-Rengifo *et al.* 2010). The Spanish sections include the Iznalloz section from the Betic Cordillera (Galbrun *et al.* 1990), the Sierra Palomera and Ariño sections (Osete *et al.* 2007) and the Almonacid De La Cuba Section (Comas-Rengifo *et al.* 2010) from the Iberian Range, central–eastern Spain. The lithology from the Spanish sections is mainly limestone, marl or mudstone (Galbrun *et al.* 1990; Comas-Rengifo *et al.* 2010).

The Mochras Toarcian succession is thicker, stratigraphically more expanded and better constrained relative to all previously studied successions, and carries a clear magnetic-polarity signal. The ammonite zones and subzones in Mochras are defined using the lowest occurrence of the respective index taxon (e.g. Callomon 1995; Simms *et al.* 2004). Zones or subzones can be determined with a high degree of accuracy in a laterally extensive, well-exposed and fossiliferous outcrop section. However, in a single borehole, such as Mochras, typically, the lowest occurrence could be

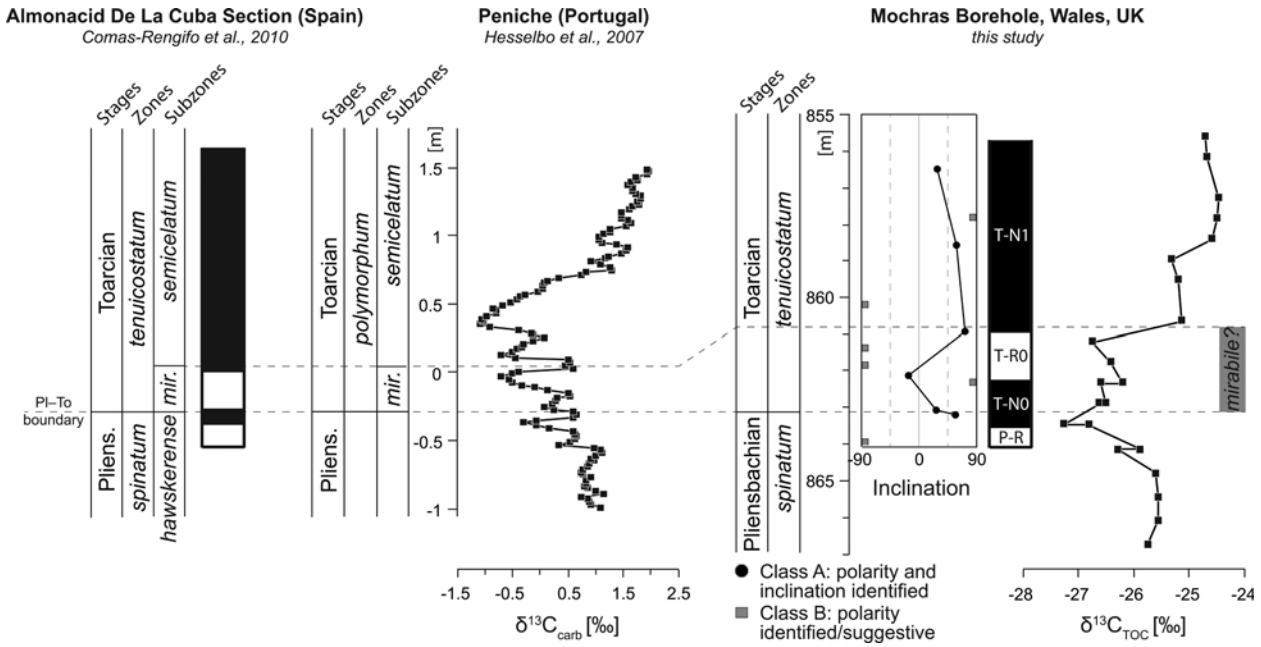

Fig. 4. Bio-, chemo- and magnetostratigraphic correlation between the Mochras core, the Peniche coastal outcrop (Portugal) and the Almonacid De La Cuba (Spain) successions (dashed lines) across the Pliensbachian–Toarcian boundary. The grey-shaded stratigraphic interval marks the potential *mirabile* Subzone in the Mochras core. Pliens., Pliensbachian; *mir.*, *mirabile*.

stratigraphically higher in the borehole compared with the surrounding rocks. The chance of an individual borehole coring a succession with the true lowest occurrence of any macrofossil is low. This drawback means that stratigraphic correlation of ammonite zone or subzone boundaries in the Mochras Borehole to outcrop sections, such as Peniche, will be somewhat approximate.

The Breggia Gorge and the Iznalloz sections are also relatively biostratigraphically complete, but are each <20 m thick (Horner & Heller 1983; Galbrun *et al.* 1990), and therefore are stratigraphically condensed relative to the Mochras core. The link between the ammonite biostratigraphic record of Breggia Gorge and the paleomagnetic record of the same section is also not well constrained. Furthermore, biostratigraphic constraints on the upper Toarcian pelagic sediments at Breggia are also relatively poor, and the Iznalloz section is incompletely exposed and subject to poorly characterized structural and/or stratigraphic discontinuities. The composite magnetic-polarity column from the Iberian Range starts within the *mirabile* Subzone of the *tenuicostatum* Zone and ends in the *illustris* Subzone of the *variabilis* Zone (Osete *et al.* 2007).

The Almonacid De La Cuba section, however, probably best characterizes the base of the Toarcian Stage among all the existing magnetic-polarity records (Comas-Rengifo *et al.* 2010; da Rocha *et al.* 2016). This section records normal magnetic polarity across the Pliensbachian–Toarcian boundary, followed by a reversed magnetic-polarity zone through most of the *mirabile* Subzone (Fig. 5; Comas-Rengifo *et al.* 2010). This reversed magnetic-polarity zone probably correlates with the stratigraphically thin T-R0 magnetozone in the Mochras core, based on chemo- and biostratigraphic correlation (Fig. 4; Hesselbo *et al.* 2007; Comas-Rengifo *et al.* 2010; da Rocha *et al.* 2016), and has also been recorded in the Iznalloz section (Galbrun *et al.* 1990). Although ammonite subzones in the *tenuicostatum* Zone have not yet been defined in the Mochras core, chemo- and magnetostratigraphic correlation between the Mochras, Peniche and the Almonacid De La Cuba successions suggests that the top of the *mirabile* Subzone equivalent is stratigraphically below *c.* 861 mbs in the Mochras core (Fig. 4).

The long normal zone (N1) in the *tenuicostatum* Zone in the Mochras core is also well documented in the magnetostratigraphic records from Iznalloz, the Iberian Range composite and Almonacid De La Cuba in Spain (Fig. 5; Galbrun *et al.* 1990; Osete *et al.* 2007; Comas-Rengifo *et al.* 2010). This normal-polarity (N1) magnetozone extends up to the lowermost *serpentinum* Zone, followed by a reversed-polarity interval (R1) in the lower *exaratum* Subzone, starting between 825 and 833 mbs in the Mochras core (Fig. 3).

The R1 magnetic reversal biostratigraphically directly matches the magnetic reversals observed at Iznalloz and in the Iberian Range (Fig. 5). Normal magnetic polarity follows the magnetic-reversal zone R1 throughout the remaining *exaratum* and lower *falciferum* subzones (Fig. 2). One sample shows reversed polarity at the *exaratum–falciferum* subzone boundary, which is therefore marked by a half-width bar. The upper *falciferum* Subzone is marked by magnetic-polarity reversal (R2), which is matched by coeval reversed magnetic polarity in the Breggia Gorge and Iznalloz sections, and the Iberian Range composite. The Breggia Gorge section contains one more reversed-polarity magnetozone in the middle of the *falciferum* Zone, which may be coeval with and has been tentatively correlated to the potential reversed interval determined by one Class A sample within the N2 magnetozone in the Mochras core (Fig. 5). This reversal has, however, not been recorded in the Iberian Range composite, and detailed magnetostratigraphic correlation to the Iznalloz section is problematic owing to its less than ideal exposure and patchy stratigraphic characterization (Fig. 5; Galbrun *et al.* 1990).

The *serpentinum–bifrons* zonal boundary is, in all studied successions, marked by normal polarity (magnetozone N3 in the Mochras core; Fig. 5). This normal magnetozone is, however, relatively thin in the Mochras core and covers only the lower *commune* Subzone of the lower *bifrons* Zone (Fig. 3). The following reversed magnetozone (R3) in the Mochras core starts halfway through the *commune* Subzone and continues through the *fibulatum* Subzone and into the upper *crassum* Subzone (all within the *bifrons* Zone; Fig. 3). In the Iberian Range, this magnetic reversal is constrained to the *bifrons* Subzone of the *bifrons* Zone (Fig. 5). This difference possibly reflects distinct biotic provincialism between different European marine basins, with diachroneity between the ammonite subzone boundaries in the *bifrons* Zone. The normal-polarity magnetozone (N4) straddles the *bifrons–variabilis* zonal

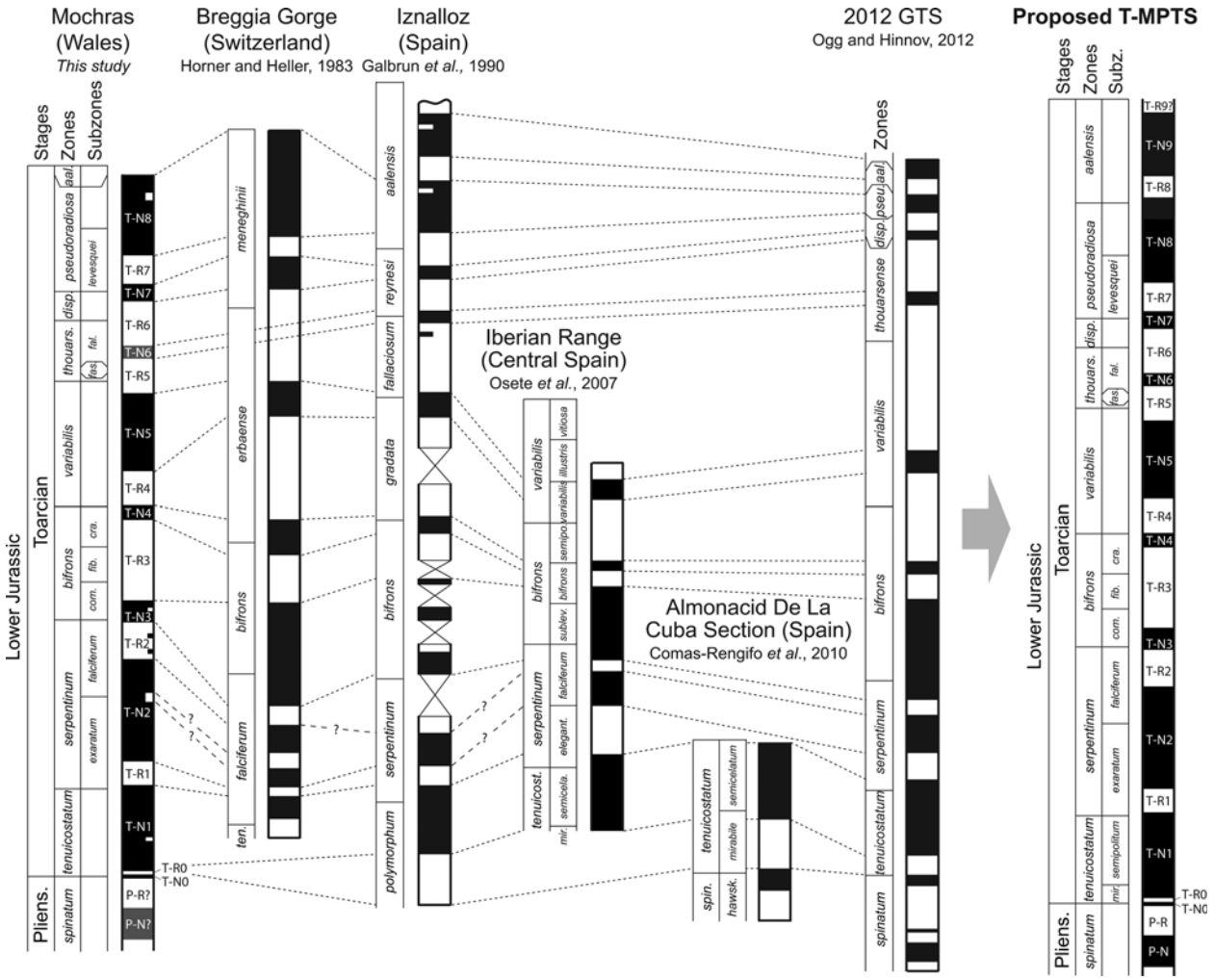

Fig. 5. Magnetostratigraphic correlations with five uppermost Pliensbachian and Toarcian successions from Europe. A proposed Toarcian magnetostratigraphic polarity timescale (T-MPTS) is shown on the right. The grey zones in the magnetostratigraphic record of the Mochras core indicate magnetozones defined as normal-polarity, only based on (at least two) Class B normal-polarity samples. The vertical scales of the bio- and magnetostratigraphy in all the five sections are proportional to the relative thickness of their ammonite zones or subzones, but not their stratigraphic thickness. The vertical scale for the Geologic Time Scale (GTS) 2012 is proportional to time. Stratigraphy in the proposed T-MPTS follows relative thickness of the Mochras core. *aal.*, *aalensis*; *com.*, *commune*; *cra.*, *crassum*; *disp.*, *dispansum*; *elegant.*, *elegantulum*; *fal.*, *fallaciosum*; *fas.*, *fascigerum*; *fib.*, *fibulatum*; *hawsk.*, *hawskerense*; *mir.*, *mirabile*; *pseu.*, *pseudoradiosa*; *semicela.*, *semicelatum*; *semipo.*, *semipolitum*; *spin.*, *spinatum;* *sublev.*, *sublevisoni*; *ten./tenuicost.*, *tenuicostatum*; *thouars.*, *thouarsense*; Pliens, Pliensbachian; Subz., Subzones.

boundary in the Mochras core and the Breggia Gorge and Iznalloz sections and is tentatively correlated with the short normal-polarity magnetozone in the upper part of the *bifrons* Zone in the Iberian Range composite (Fig. 5). Minor differences in the biostratigraphic position of the N4 magnetozone in the different European successions possibly also indicate diachroneity for the *bifrons–variabilis* zonal boundary, or alternatively, may reflect a historical difference in the definition of the base of the *variabilis* Zone, depending on either the first occurrence of *Haugia* or the last occurrence of *Hildoceras semipolitum/Catacoeloceras* spp. (Page 2003).

Magnetostratigraphic correlation of intervals above the *bifrons* Zone is less precise because of the less well-constrained biostratigraphic correlation between different European ammonite provinces and associated ammonite zonal boundaries. The *erbaense* and *meneghinii* zones in the Breggia Gorge section probably equate to the *variabilis–thouarsense* and the *pseudoradiosa–aalensis* (*levesquei*) zones in NW Europe, as recorded in the Mochras core (Page 2003). In the Iznalloz section, the *gradata* Zone is the equivalent of the NW European *variabilis* Zone, the *fallaciosum* Zone is probably partly coeval with the NW European *thouarsense* Zone, and the *reynesi* Zone is probably partly coeval with the NW European *dispansum* Zone (Page 2003). The integrated stratigraphic framework proposed here for the upper Toarcian therefore follows the correlation between the local palaeomagnetic-polarity records, with due consideration of the ammonite biostratigraphy (Fig. 5). The upper Toarcian magnetic-polarity record of the Mochras core closely resembles the GTS2012 composite record. The thickness of the *pseudoradiosa* Zone in the Mochras core is larger than might be expected if sedimentation rates were constant and the duration of the zone in the GTS2012 were correct (Fig. 5). The precise onset and termination of magnetic-polarity reversals in the different upper Toarcian sedimentary successions, relative to ammonite zonal boundaries, is also not always consistent (Fig. 5). This difference potentially suggests that diachroneity between ammonite zonal boundaries in different biological (ammonite) provinces complicates high-resolution biostratigraphic correlation, not only in the middle, but also in the upper Toarcian. The uppermost subdivision of the Toarcian in the Mochras core, the *aalensis* Zone, is very thin (*c.* 3 m) owing to truncation at the top, and no palaeomagnetic samples were analysed. The *aalensis* Zone in the Iznalloz section is marked by two further palaeomagnetic reversals (Fig. 5; Galbrun *et al.* 1990; Ogg & Hinnov 2012).

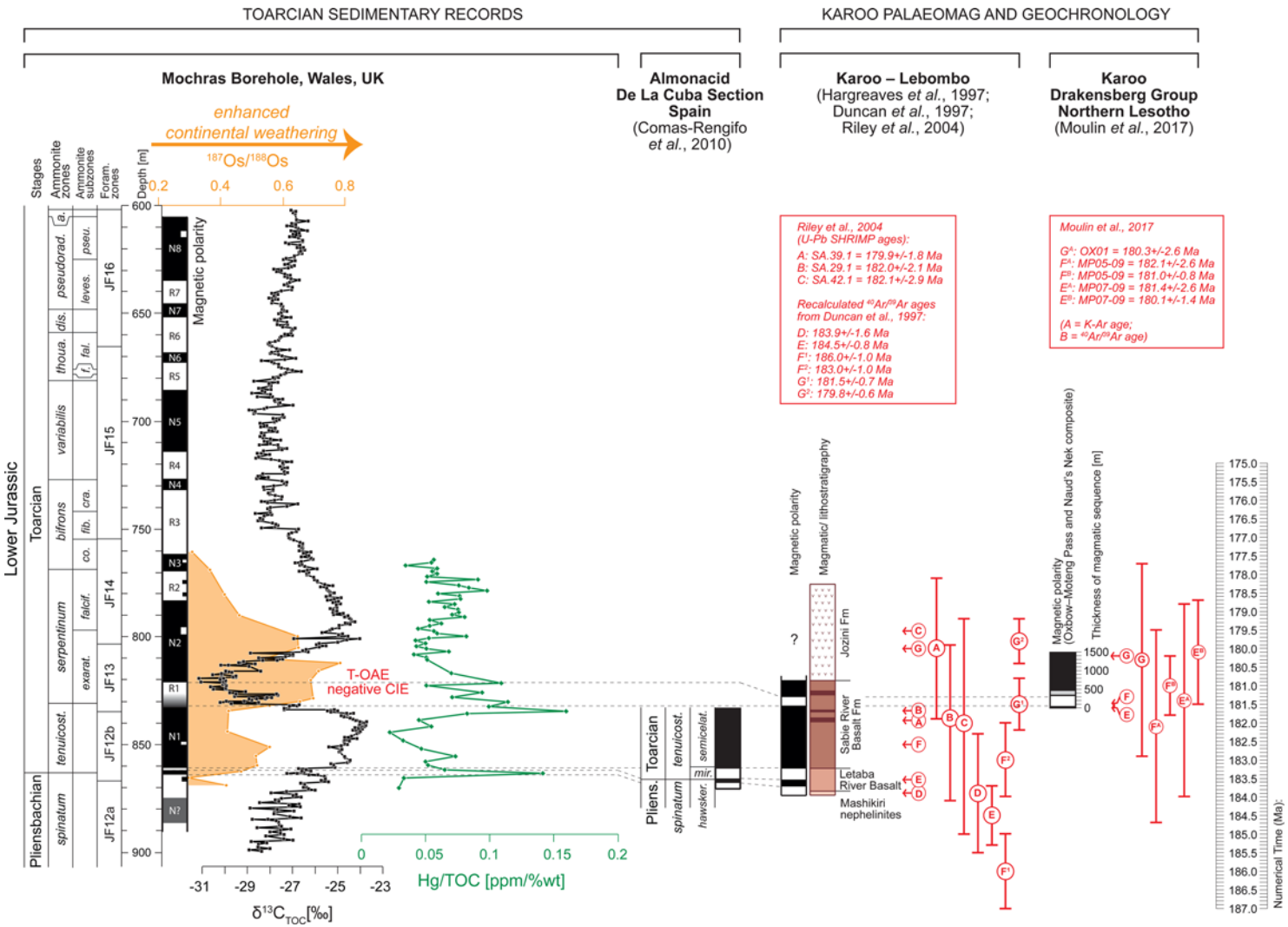

Fig. 6. Magnetostratigraphic correlation between the Mochras core (this study), the Almonacid De La Cuba Section in Spain (Comas-Rengifo *et al.* 2010) and the Karoo volcanic rocks at Lebombo and northern Lesotho in South Africa (Duncan *et al.* 1997; Hargreaves *et al.* 1997; Riley *et al.* 2004; Comas-Rengifo *et al.* 2010; Moulin *et al.* 2017). The lithological column of the Lebombo and northern Lesotho Drakensberg regions from the bottom to the top contains the Mashikiri Nephelinite, the Letaba Picrite, the Sabie River Basalt and Jozini Rhyolite (Hargreaves *et al.* 1997). The radioisotopic ages from Lebombo are from Riley *et al.* (2004) and recalculated from Duncan *et al.* (1997). The stratigraphic levels of the analysed samples are indicated by the arrowed letters A–G (F^1 and F^2 and G^1 and G^2 indicate different samples within level F and level G, respectively), with the uncertainty bars representing the age defined by U–Pb and $^{40}Ar/^{39}Ar$ dating. The high-resolution bulk organic-carbon isotope record (Xu *et al.* 2018) and the Hg–TOC record (Percival *et al.* 2015, 2016) from the Mochras core illustrate the carbon-cycle perturbation and the fingerprint of enhanced volcanism at the Pliensbachian–Toarcian boundary and the T-OAE. *a.*, *aalensis*; *co.*, *commune*; *cra.*, *crassum*; *dis.*, *dispansum*; *exarat.*, *exaratum*; *falcif.*, *falciferum*; *fal.*, *fallaciosum*; *f.*, *fascigerum*; *fib.*, *fibulatum*; *hawsk.*, *hawskerense*; *leves.*, *levesquei*; *mir.*, *mirabile*; *pseudorad/pseu.*, *pseudoradiosa*; *semicelat.*, *semicelatum*; *tenuicost.*, *tenuicostatum*; *thoua.*, *thouarsense*.

Proposed geomagnetic polarity timescale for the Toarcian Stage (T-MPTS)

A geomagnetic polarity timescale for the entire Toarcian Stage is proposed based on the new data from the Mochras core, integrated with previously published data (Fig. 5). The *mirabile* Subzone (*tenuicostatum* Zone) is marked in the proposed T-MPTS to indicate the position of the R0 magnetozone, based on data from Almonacid De La Cuba (Comas-Rengifo *et al.* 2010). The base of the R1 magnetozone is placed above the base of the *exaratum* Subzone, according to the results of the Iznalloz section and the Iberian Range composite (Galbrun *et al.* 1990; Osete *et al.* 2007). The R8 and N9 magnetozones in the *aalensis* Zone, which are not recorded in the Mochras core, are added at the top of the column following the Iznalloz section (Galbrun *et al.* 1990).

The relative stratigraphic thicknesses of the Toarcian ammonite zones differ between sections, and from those defined in GTS2012. The relative stratigraphic thicknesses of the Toarcian ammonite zones used for the T-MPTS proposed here reflect a combination of the relative stratigraphic thicknesses of the zones in the Mochras core and the data as represented in GTS2012 (Fig. 5). Assuming constant sedimentation rates, the *serpentinum* and *pseudoradiosa* zones are relatively longer and the *bifrons*, *variabilis* and *thouarsense* zones are relatively shorter in duration in the Mochras core, compared with GTS2012 (Fig. 5). This difference may suggest either changes in sedimentation rate throughout the Toarcian in the Mochras core or a disproportionate representation of thickness relative to time in GTS2012, resulting from changes in sedimentation rate within, or between, the Iznalloz, Iberian Range and Almonacid De La Cuba sections in Spain. Because the duration of some, especially the middle and upper, Toarcian zones is not yet accurately determined, future integration with astrochronological and geochronological data is required to accurately and precisely constrain the relative and numerical Toarcian timescale.

Linking Karoo–Ferrar volcanism with the Toarcian OAE

The carbon-cycle perturbations at the Pliensbachian–Toarcian boundary and in the early Toarcian have been linked to the Karoo–Ferrar Large Igneous Province and associated release of volcanogenic CO_2 and methane from biogenic sources and subseafloor clathrates (Duncan *et al.* 1997; McElwain *et al.* 2005; Svensen *et al.* 2007; Percival *et al.* 2015, 2016). Elevated sedimentary mercury concentrations at the Pliensbachian–Toarcian boundary and in sedimentary intervals recording the T-OAE further suggested enhanced volcanic activity at these times (Percival *et al.* 2015, 2016). A temporal link between Karoo–Ferrar basalt emplacement and the T-OAE was previously suggested based on radio-isotopic dating of surface basalts and dykes and sills from this Large Igneous Province, and volcanic ashes interbedded in sedimentary successions with ammonite biostratigraphy (e.g. Sell *et al.* 2014; Burgess *et al.* 2015). The precise timing of Karoo–Ferrar volcanism and its relationship to the T-OAE are, however, not well constrained owing to (1) substantial uncertainties on earlier radio-isotopic Ar–Ar ages and (2) poor bio- and chemostratigraphic control on those marine strata that have yielded accurate and precise U–Pb ages from interbedded volcaniclastic deposits.

High-resolution integrated magnetostratigraphic data from the marine realm may potentially be correlated with the geomagnetic polarity record obtained from the Karoo successions of South Africa (Hargreaves *et al.* 1997). The onset of accumulation of the Karoo volcanic succession was previously correlated with the Pliensbachian–Toarcian boundary interval at Almonacid De La Cuba, Spain, based on magnetostratigraphy (da Rocha *et al.* 2016). Bio- and magnetostratigraphic correlation of the Pliensbachian–Toarcian boundary between the Mochras succession and Almonacid De La Cuba, and subsequent magnetostratigraphic correlation to the Karoo volcanic succession from the Lebombo volcanic rift margin and the Drakensberg Group in northern Lesotho, southern Africa, suggests that the three normal-polarity magnetozones there correspond to the N1 and N2 magnetozones in the Mochras core (Fig. 6; Hargreaves *et al.* 1997; Riley *et al.* 2004; Comas-Rengifo *et al.* 2010; da Rocha *et al.* 2016). The youngest normal-polarity magnetozone in the Lebombo succession, which may correlate with the N2 magnetozone in the Mochras core, is less thick than the preceding normal-polarity magnetozone in the same sequence (Fig. 6). The N1 and N2 normal-polarity zones have a comparable thickness in the Mochras core. This difference may be explained by a combined effect of the changing sedimentation rate at Mochras and the relatively sporadic and variable accumulation rates of the Karoo lava flows.

Based on this correlation, emplacement of the Karoo Large Igneous Province had already begun in the late Pliensbachian, and continued until after the T-OAE negative CIE. Basalt emplacement in the Karoo Basin of South Africa might actually have persisted throughout the duration of the early Toarcian overarching positive CIE, which possibly linked to prolonged and large-scale extraction of ^{13}C-depleted carbon from the global ocean–atmosphere system, brought about by elevated atmospheric pCO_2 and associated prolonged climatic and oceanographic change at that time. The T-OAE negative CIE, superimposed on the overarching early Toarcian positive CIE, possibly reflects the time of maximum isotopically light carbon injection either directly from Karoo–Ferrar basalt degassing or through additional processes such as thermogenic carbon release from subsurface organic-rich shales, or through the initiation of positive feedback mechanisms in Earth's climate system, with, for example, the release of carbon from seafloor methane clathrates.

Conclusions

A high-resolution magnetostratigraphic record is presented, spanning the complete Toarcian succession of the Mochras Borehole, Wales, and providing a bio- and chemostratigraphically integrated and refined geomagnetic polarity timescale for the Toarcian Stage (T-MPTS). The combined bio- (ammonite, foraminifer), chemo- (carbon-isotope) and magnetostratigraphic framework for the entire Toarcian Stage forms an important reference record for future correlations between global marine, and marine and terrestrial successions. This framework also provides new accurate and precise correlations with the basalt lava sequence of the Karoo Large Igneous Province, linking the Pliensbachian–Toarcian boundary and T-OAE climatic and environmental perturbations directly to this episode of major volcanic activity.

Acknowledgements All authors thank the British Geological Survey (BGS), especially T. Gallagher and S. Renshaw, for allowing access to the Mochras core. C. V. Ullmann is acknowledged for the help with sampling and the general discussion. J.B.R. publishes with the approval of the Executive Director of the British Geological Survey (NERC). This paper is a contribution to IGCP 655 (IUGS-UNESCO): 'Toarcian Oceanic Anoxic Event: Impact on marine carbon cycle and ecosystems', and IGCP 632 (IUGS-UNESCO): 'Continental Crises of the Jurassic: Major Extinction Events and Environmental Changes within Lacustrine Ecosystems'.

Funding We acknowledge funding from Shell International Exploration & Production B.V., the International Continental Scientific Drilling Program (ICDP) and the Natural Environmental Research Council (NERC) (grant number NE/N018508/1).

Scientific editing by Graham Shields-Zhou

References

Al-Suwaidi, A.H., Angelozzi, G.N. *et al.* 2010. First record of the Early Toarcian Oceanic Anoxic Event from the Southern Hemisphere, Neuquén Basin,

Argentina. *Journal of the Geological Society, London*, **167**, 633–636, https://doi.org/10.1144/0016-76492010-025

Al-Suwaidi, A.H., Hesselbo, S.P. *et al.* 2016. The Toarcian Oceanic Anoxic Event (Early Jurassic) in the Neuquén Basin, Argentina: a reassessment of age and carbon isotope stratigraphy. *Journal of Geology*, **124**, 171–193.

Bodin, S., Krencker, F.-N., Kothe, T., Hoffmann, R., Mattioli, E., Heimhofer, U. & Kabiri, L. 2016. Perturbation of the carbon cycle during the late Pliensbachian–early Toarcian: New insight from high-resolution carbon isotope records in Morocco. *Journal of African Earth Sciences*, **116**, 89–104.

Boulila, S., Galbrun, B., Huret, E., Hinnov, L.A., Rouget, I., Gardin, S. & Bartolini, A. 2014. Astronomical calibration of the Toarcian Stage: Implications for sequence stratigraphy and duration of the early Toarcian OAE. *Earth and Planetary Science Letters*, **386**, 98–111.

Burgess, S.D., Bowring, S.A., Fleming, T.H. & Elliot, D.H. 2015. High-precision geochronology links the Ferrar large igneous province with early-Jurassic oceanic anoxia and biotic crisis. *Earth and Planetary Science Letters*, **415**, 90–99.

Callomon, J.H. 1995. Time from fossils: S. S. Buckman and Jurassic high-resolution geochronology. *In*: Le Bas, M.J. (ed.) *Milestones in Geology*. Geological Society, London, Memoirs, **16**, 127–150, https://doi.org/10.1144/GSL.MEM.1995.016.01.14

Cohen, A.S., Coe, A.L., Harding, S.M. & Schwark, L. 2004. Osmium isotope evidence for the regulation of atmospheric CO_2 by continental weathering. *Geology*, **32**, 157–160.

Comas-Rengifo, M.J., Arias, C., Gómez, J.J., Goy, A., Herrero, C., Osete, M.L. & Palencia, A. 2010. A complementary section for the proposed Toarcian (Lower Jurassic) global stratotype: the Almonacid De La Cuba section (Spain). *Stratigraphy and Geological Correlation*, **18**, 133–152.

Copestake, P. & Johnson, B. 2014. *Lower Jurassic foraminifera from the Llanbedr (Mochras Farm) Borehole, North Wales, UK*. Monograph of the Palaeontographical Society, **167**.

Danise, S., Twitchett, R.J., Little, C.T.S. & Clémence, M.-E. 2013. The impact of global warming and anoxia on marine benthic community dynamics: an example from the Toarcian (Early Jurassic). *PLoS ONE*, **8**, e56255, https://doi.org/10.1371/journal.pone.0056255

Danise, S., Twitchett, R.J. & Little, C.T.S. 2015. Environmental controls on Jurassic marine ecosystems during global warming. *Geology*, **43**, 263–266.

da Rocha, R.B., Mattioli, E. *et al.* 2016. Base of the Toarcian Stage of the Lower Jurassic defined by the Global Boundary Stratotype Section and Point (GSSP) at the Peniche section (Portugal). *Episodes*, **39**, 460–481.

Dera, G., Neige, P., Dommergues, J.-L. & Brayard, A. 2011. Ammonite paleobiogeography during the Pliensbachian–Toarcian crisis (Early Jurassic) reflecting paleoclimate, eustasy, and extinctions. *Global and Planetary Change*, **78**, 92–105.

Dobson, M.R. & Whittington, R.J. 1987. The geology of Cardigan Bay. *Proceedings of the Geologists' Association*, **98**, 331–353.

Duncan, R.A., Hooper, P.R., Rehacek, J., Marsh, J.S. & Duncan, A.R. 1997. The timing and duration of the Karoo igneous event, southern Gondwana. *Journal of Geophysical Research*, **102**, 18127–18138.

French, K.L., Sepúlveda, J., Trabucho-Alexandre, J., Gröcke, D.R. & Summons, R.E. 2014. Organic geochemistry of the early Toarcian oceanic anoxic event in Hawsker Bottoms, Yorkshire, England. *Earth and Planetary Science Letters*, **390**, 116–127.

Galbrun, B., Gabilly, J. & Rasplus, L. 1988. Magnetostratigraphy of the Toarcian stratotype sections at Thouars and Airvault (Deux-Sèvres, France). *Earth and Planetary Science Letters*, **87**, 453–462.

Galbrun, B., Baudin, F., Fourcade, E. & Rivas, P. 1990. Magnetostratigraphy of the Toarcian Ammonitico Rosso limestone at Iznalloz, Spain. *Geophysical Research Letters*, **17**, 2441–2444.

Gill, C.B., Lyons, T.W. & Jenkyns, H.C. 2011. A global perturbation to the sulfur cycle during the Toarcian Oceanic Anoxic Event. *Earth and Planetary Science Letters*, **312**, 484–496.

Hargreaves, R.B., Rehacek, J. & Hooper, P.R. 1997. Paleomagnetism of the Karoo igneous rocks in South Africa. *South African Journal of Geology*, **100**, 195–212.

Hermoso, M., Callonnec, L.L., Minoletti, F., Renard, M. & Hesselbo, S.P. 2009. Expression of the Early Toarcian negative carbon-isotope excursion in separated carbonate microfractions (Jurassic, Paris Basin). *Earth and Planetary Science Letters*, **277**, 194–203.

Hesselbo, S.P., Gröcke, D.R., Jenkyns, H.C., Bjerrum, C.J., Farrimond, P., Bell, H.S.M. & Green, O.R. 2000. Massive dissociation of gas hydrate during a Jurassic oceanic anoxic event. *Nature*, **406**, 392–395.

Hesselbo, S.P., Jenkyns, H.C., Duarte, L.V. & Oliveira, L.C.V. 2007. Carbon-isotope record of the Early Jurassic (Toarcian) Oceanic Anoxic Event from fossil wood and marine carbonate (Lusitanian Basin, Portugal). *Earth and Planetary Science Letters*, **253**, 455–470.

Hesselbo, S.P., Bjerrum, C.J. *et al.* 2013. Mochras borehole revisited: a new global standard for Early Jurassic earth history. *Scientific Drilling*, **16**, 81–91.

Horner, F. & Heller, F. 1983. Lower Jurassic magnetostratigraphy at the Breggia Gorge (Ticino, Switzerland) and Alpe Turati (Como, Italy). *Geophysical Journal of the Royal Astronomical Society*, **73**, 705–718.

Iglesia Llanos, M.P. & Riccardi, A.C. 2000. The Neuquén composite section: magnetostratigraphy and biostratigraphy of the marine lower Jurassic from the Neuquén basin (Argentina). *Earth and Planetary Science Letters*, **181**, 443–457.

Ivimey-Cook, H.C. 1971. Stratigraphical palaeontology of the Lower Jurassic of the Llanbedr (Mochras Farm) Borehole. *In*: Woodland, A.W. (ed.) *The Llanbedr (Mochras Farm) Borehole*. Institute of Geological Sciences Report, **771/18**, 87–92.

Jenkyns, H.C. 1985. The Early Toarcian and Cenomanian–Turonian anoxic events in Europe: comparisons and contrasts. *International Journal of Earth Sciences*, **74**, 505–518.

Jenkyns, H.C. 1988. The early Toarcian (Jurassic) anoxic event: Stratigraphic, sedimentary, and geochemical evidence. *American Journal of Science*, **288**, 101–151.

Jenkyns, H.C. 2003. Evidence for rapid climate change in the Mesozoic–Palaeogene greenhouse world. *Philosophical Transactions of the Royal Society of London, Series A*, **361**, 1885–1916.

Jenkyns, H.C. 2010. Geochemistry of oceanic anoxic events. *Geochemistry, Geophysics, Geosystems*, **11**, Q03004, https://doi.org/10.1029/2009GC002788

Jenkyns, H.C. & Clayton, C.J. 1997. Lower Jurassic epicontinental carbonates and mudstones from England and Wales: chemostratigraphic signals and the early Toarcian anoxic event. *Sedimentology*, **44**, 687–706.

Jenkyns, H.C., Gröcke, D.R. & Hesselbo, S.P. 2001. Nitrogen isotope evidence for water mass denitrification during the early Toarcian (Jurassic) oceanic anoxic event. *Paleoceanography*, **16**, 593–603.

Jenkyns, H.C., Jones, C.E., Gröcke, D.R., Hesselbo, S.P. & Parkinson, D.N. 2002. Chemostratigraphy of the Jurassic System: applications, limitations and implications for palaeoceanography. *Journal of the Geological Society, London*, **159**, 351–378, https://doi.org/10.1144/0016-764901-130

Katz, M.E., Wright, J.D., Miller, K.G., Cramer, B.S., Fennel, K. & Falkowski, P.G. 2005. Biological overprint of the geological carbon cycle. *Marine Geology*, **217**, 323–338.

Kemp, D.B., Coe, A.L., Cohen, A.S. & Schwark, L. 2005. Astronomical pacing of methane release in the Early Jurassic period. *Nature*, **437**, 396–399.

Kirschvink, J.L. 1980. The least-squares line and plane and the analysis of palaeomagnetic data. *Geophysical Journal of the Royal Astronomical Society*, **62**, 699–718.

Kodama, K.P. 2012. Inclination shallowing in sedimentary rocks: evidence, mechanism and cause. *In*: Kodama, K.P. (ed.) *Paleomagnetism of Sedimentary Rocks: Process and Interpretation*, 1st edn. Blackwell, Oxford, 34–45.

Korte, C., Hesselbo, S.P., Ullmann, C.V., Dietl, G., Ruhl, M., Schweigert, G. & Thibault, N. 2015. Jurassic climate mode governed by ocean gateway. *Nature Communications*, https://doi.org/10.1038/ncomms10015

Littler, K., Hesselbo, S.P. & Jenkyns, H.C. 2010. A carbon-isotope perturbation at the Pliensbachian–Toarcian boundary: evidence from the Lias Group, NE England. *Geological Magazine*, **147**, 181–192.

Martindale, R.C. & Aberhan, M. 2017. Response of macrobenthic communities to the Toarcian Oceanic Anoxic Event in northeastern Panthalassa (Ya Ha Tinda, Alberta, Canada). *Palaeogeography, Palaeoclimatology, Palaeoecology*, **478**, 103–120.

McArthur, J.M., Steuber, T., Page, K.N. & Landman, N.H. 2016. Sr-isotope stratigraphy: Assigning time in the Campanian, Pliensbachian, Toarcian, and Valanginian. *Journal of Geology*, **124**, 569–586.

McElwain, J.C., Wade-Murphy, J. & Hesselbo, S.P. 2005. Changes in carbon dioxide during an oceanic anoxic event linked to intrusion into Gondwana coals. *Nature*, **435**, 479–482.

McFadden, P.L. & Reid, A.B. 1982. Analysis of paleomagnetic inclination data. *Geophysical Journal of the Royal Astronomical Society*, **69**, 307–319.

Moulin, M., Fluteau, F., Courtillot, V., Marsh, J., Delpech, G., Quidelleur, X. & Gérard, M. 2017. Eruptive history of the Karoo lava flows and their impact on early Jurassic environmental change. *Journal of Geophysical Research: Solid Earth*, **122**, 738–772.

Müller, R.D., Seton, M. *et al.* 2016. Ocean basin evolution and global-scale plate reorganisation events since Pangea breakup. *Annual Review of Earth and Planetary Sciences*, **44**, 107–138.

Newton, R.J., Reeves, E.P., Kafousia, N., Wignall, P.B., Bottrell, S.H. & Sha, J.-G. 2011. Low marine sulfate concentrations and the isolation of the European epicontinental sea during the Early Jurassic. *Geology*, **39**, 7–10.

Ogg, J.G. & Hinnov, L.A. 2012. Jurassic. *In*: Gradstein, F.M., Ogg, J.G., Schmitz, M.D. & Ogg, G.M. (eds) *The Geologic Time Scale 2012*. Elsevier, Amsterdam, 731–791.

Osete, M.-L., Gialanella, P.-R., Gómez, J.J., Villalaín, J.J., Goy, A. & Heller, F. 2007. Magnetostratigraphy of Early–Middle Toarcian expanded sections from the Iberian Range (central Spain). *Earth and Planetary Science Letters*, **259**, 319–332.

Page, K.N. 2003. The Lower Jurassic of Europe: its subdivision and correlation. *In*: Ineson, J.R. & Surlyk, F. (eds) *The Jurassic of Denmark and Greenland*. Geological Survey of Denmark and Greenland Bulletin, **1**, 23–59.

Pálfy, J. & Smith, P.L. 2000. Synchrony between Early Jurassic extinction, oceanic anoxic event, and the Karoo–Ferrar flood basalt volcanism. *Geology*, **28**, 747–750.

Pearson, P.N. & Thomas, E. 2015. Drilling disturbance and constraints on the onset of the Paleocene–Eocene boundary carbon isotope excursion in New Jersey. *Climate of the Past*, **11**, 95–104.

Percival, L.M.E., Witt, M.L.I. *et al.* 2015. Globally enhanced mercury deposition during the end-Pliensbachian and Toarcian OAE: A link to the Karoo–Ferrar Large Igneous Province. *Earth and Planetary Science Letters*, **428**, 267–280.

Percival, L.M.E., Cohen, A.S. *et al.* 2016. Osmium isotope evidence for two pulses of increased continental weathering linked to Early Jurassic volcanism and climate change. *Geology*, **44**, 759–762.

Riley, T.R., Millar, I.L., Watkeys, M.K., Curtis, M.L., Leat, P.T., Klausen, M.B. & Fanning, C.M. 2004. U–Pb zircon (SHRIMP) ages for the Lebombo rhyolites, South Africa: refining the duration of Karoo volcanism. *Journal of the Geological Society, London*, **161**, 547–550, https://doi.org/10.1144/0016-764903-181

Rita, P., Reolid, M. & Duarte, L.V. 2016. Benthic foraminiferal assemblages record major environmental perturbations during the Late Pliensbachian–Early Toarcian interval in the Peniche GSSP, Portugal. *Palaeogeography, Palaeoclimatology, Palaeoecology*, **454**, 267–281.

Ruhl, M., Hesselbo, S.P. *et al.* 2016. Astronomical constraints on the duration of the Early Jurassic Pliensbachian Stage and global climatic fluctuations. *Earth and Planetary Science Letters*, **455**, 149–165.

Satolli, S., Turtù, A. & Donatelli, U. 2015. Magnetostratigraphy of the Salto del Cieco section (Northern Apennines, Italy) from the Pliensbachian to Jurassic/Cretaceous boundary. *Newsletters on Stratigraphy*, **48/2**, 153–177.

Sælen, G., Tyson, R.V., Telnæs, N. & Talbot, M.R. 2000. Contrasting watermass conditions during deposition of the Whitby Mudstone (Lower Jurassic) and Kimmeridge Clay (Upper Jurassic) formations, UK. *Palaeogeography, Palaeoclimatology, Palaeoecology*, **163**, 163–196.

Schouten, S., van Kaam-Peters, H.M.E., Rijpstra, W.I.C., Schoell, M. & Sinninghe-Damsté, J.S. 2000. Effects of an Oceanic Anoxic Event on the stable carbon isotopic composition of Early Toarcian Carbon. *American Journal of Science*, **300**, 1–22.

Sell, B., Ovtcharova, M. *et al.* 2014. Evaluating the temporal link between the Karoo LIP and climatic–biologic events of the Toarcian Stage with high-precision U–Pb geochronology. *Earth and Planetary Science Letters*, **408**, 48–56.

Sellwood, B.W. & Jenkyns, H.C. 1975. Basins and swells and the evolution of an epeiric sea (Pliensbachian–Bajocian of Great Britain). *Journal of the Geological Society, London*, **131**, 373–388, https://doi.org/10.1144/gsjgs.131.4.0373

Simms, M.J., Chidlaw, N., Morton, N. & Page, K.N. 2004. *British Lower Jurassic Stratigraphy*. Geological Conservation Review Series, **30**. Joint Nature Conservation Committee, Peterborough.

Suan, G., van de Schootbrugge, B., Adatte, T., Fiebig, J. & Oschmann, W. 2015. Calibrating and magnitude of the Toarcian carbon cycle perturbation. *Paleoceanography*, **30**, PA2758.

Svensen, H., Planke, S., Chevallier, L., Malthe-Sorenssen, A., Corfu, F. & Jamtveit, B. 2007. Hydrothermal venting of greenhouse gases triggering Early Jurassic global warming. *Earth and Planetary Science Letters*, **256**, 554–566.

Tappin, D.R., Chadwick, R.A., Jackson, A.A., Wingfield, R.T.R. & Smith, N.J.P. 1994. *Geology of Cardigan Bay and the Bristol Channel, United Kingdom*. Offshore Regional Report, British Geological Survey. HMSO, London.

Torsvik, T.H., Van der Voo, R. *et al.* 2012. Phanerozoic polar wander, palaeogeography and dynamics. *Earth-Science Reviews*, **114**, 325–368.

Ullmann, C.V., Thibault, N.R., Ruhl, M., Hesselbo, S.P. & Korte, C. 2014. Effect of a Jurassic oceanic anoxic event on belemnite ecology and evolution. *Proceedings of the National Academy of Sciences of the USA*, **111**, 10073–10076.

van de Schootbrugge, B., Bailey, T.R., Katz, M.E., Wright, J.D., Rosenthal, Y., Feist-Burkhardt, S. & Falkowski, P.G. 2005. Early Jurassic climate change and the radiation of organic walled phytoplankton in the Tethys Sea. *Paleobiology*, **31**, 73–97.

Woodland, A.W. (ed.) 1971. *The Llanbedr (Mochras Farm) Borehole*. Institute of Geological Sciences, Report, **71/18**, 27–28.

Xu, W., Ruhl, M. *et al.* 2017. Carbon sequestration in an expanded lake system during the Toarcian Oceanic Anoxic Event. *Nature Geoscience*, **10**, 129–134.

Xu, W., Ruhl, M. *et al.* 2018. Evolution of the Toarcian (Early Jurassic) carbon-cycle and global climatic controls on local sedimentary processes (Cardigan Bay Basin, UK). *Earth and Planetary Science Letters*, **484**, 396–411.